Spatial-Angular Analysis of Displays for Reproduction of Light Fields

Amir Said[a] and Eino-Ville Talvala[b]

[a]Hewlett-Packard Laboratories, Palo Alto, CA, USA
[b]Electrical Engineering Dept., Stanford University, Stanford, CA, USA

ABSTRACT

From a signal processing perspective, we examine the main factors defining the visual quality of autostereoscopic 3-D displays, which are beginning to reproduce the plenoptic function with increasing accuracy. We propose using intuitive visual tools and ray-tracing simulations to gain insight into the signal processing aspects, and we demonstrate the advantages of analyzing what we call mixed spatial-angular spaces. With this approach we are able to intuitively demonstrate some basic limitations of displays using anisotropic diffusers or lens arrays. Furthermore, we propose new schemes for improved performance.

Keywords: Light field, plenoptic function, autostereo displays, image processing, spatial-angular resolution

1. INTRODUCTION

As display technologies advance, we can foresee autostereo devices reproducing three-dimensional scenes, for multiple observers and without special viewing apparatus, through increasingly more accurate reproductions of light fields. While there are many different approaches to achieve this goal, which are described in several books and surveys,[1–6] a major challenge to newcomers to this research field is to sort out the different characteristics of each method. It is easy to start focusing too much on issues related to current technologies and implementations, and not consider the fundamental problems that are inherent to a method, nor being able to recognize techniques that may be more or less promising in the long term.

Another common difficulty comes from the fact that a 3-D display is meant to be viewed from different angles, and that the quality of the observed image keeps changing with viewer position, possibly in a non-smooth manner. Thus, photos of display prototypes convey very limited information about how well the device reproduces natural 3-D views, and how convincing and pleasing the viewing experience is. Video can convey significantly more information, but its use is still not very common, and it is much harder to publish and maintain.

We also observe that there is very active research on capturing and rendering of light fields (in 2-D), with possible applications to computational photography,[7] but there has been less work on the application of that research to full reproduction (3-D display) of light fields. There are many difficulties in translating well-known image/video processing properties—like pixelation and aliasing—into intuition about 3-D display visual quality.

Considering these problems, in this work we present the following contributions to the study of displays capable of reproducing light fields:

- We discuss how images created from a type of mathematical representation, which we call *spatial-angular images,* provide rich and intuitive visual information for analysis of some fundamental factors that determine the quality of the reproduced 3-D views, and thus also the overall quality of a type of display.
- Using properties of spatial-angular images, we demonstrate that even a simple analysis of view distortion can show why, for different types of displays, the quality of the reproduction must depend on the depth of the reproduced objects in relation to the display plane.

Author e-mail addresses: amir_said@hp.com, talvala@stanford.edu

- We use ray-tracing simulations of displays to create realistic views of different systems. This makes it easy to show how different parameters change the view quality and type of visual artifacts, enabling more intuitive understanding of the different factors and trade-offs. Furthermore, simulation allows us to temporarily disregard physical laws. For example, it is interesting to know how a display would look when lens aberration is completely eliminated.

We also propose new approaches to designing better displays which exploit how new digital projectors, display technologies, and powerful computers allow us to ignore design constraints that were essential in the analog domain.

- Displays that use lens arrays and diffused light modulators at the focal plane commonly have a spatial view resolution (pixels per unit length) roughly identical to the lens size, and thus very small lenses are needed to avoid pixelation. We show that by changing amount of diffusion and employing multiple projectors the spatial resolution can be several times larger than that defined by lens size.
- We extend the ideas of the modification above, showing that it can be considered only a particular solution, in a much larger set of possible schemes for creating 3-D displays. New technology enables us to move to a new paradigm, where instead of thinking about combining traditional imaging optics, we can instead use multiple light modulators combined with elements for light diffusion, refraction or reflection (not necessarily lenses), to re-create the four-dimensional light field of a scene. This requires hardware, now becoming available, that is able to manage and compute the huge amounts of information required to map the desired light field rays to the inputs of the light modulators.

All the analyses and techniques presented in this work are applicable to displays that present parallax in both the horizontal and vertical direction. However, to simplify the notation and explanations, we show examples of displays with parallax in the horizontal direction only.

2. SPATIAL-ANGULAR IMAGES

We follow the terminology for light ray distribution used by Adelson and Bergen,[8] and call the function describing the distribution of light radiance in space the *plenoptic function.* The original definition includes time and light wavelength as parameters, which we consider implicitly to simplify the notation. Thus, we assume that radiance in a point in space $\mathbf{a} = (x, y, z)$, propagating along direction $\mathbf{d}(\phi, \theta) = (\sin\phi\cos\theta, \sin\phi\sin\theta, \cos\phi)$, is defined by the five-dimensional function

$$p_{\mathrm{g}}(x, y, z, \phi, \theta),$$

with $\phi \in [0, \pi]$ and $\theta \in [0, 2\pi)$ corresponding to variables of standard spherical coordinate systems.

In a transparent medium the plenoptic function has a certain amount of redundancy because radiance is conserved, i.e.,

$$p_{\mathrm{g}}(x, y, z, \phi, \theta) = p_{\mathrm{g}}(x + \alpha\sin\phi\cos\theta, y + \alpha\sin\phi\sin\theta, z + \alpha\cos\phi, \phi, \theta), \tag{1}$$

for all values of α that correspond to unoccluded points in a transparent medium.

When studying an apparatus that is meant to recreate the plenoptic function in a surface, it is convenient to assume that the display is in plane $z = 0$. In this case, we define the display's plenoptic function as

$$p_{\mathrm{s}}(x, y, \phi, \theta) = p^{*}_{\mathrm{g}}(x, y, 0, \phi, \theta), \tag{2}$$

where the asterisk is used to indicate that the radiance values are equal to the plenoptic function in unoccluded parts of the display, and inside virtual objects and in the occluded parts by values extrapolated using eq. (1).

Note that this function has two *spatial dimensions* (x, y) and two *angular dimensions* (ϕ, θ), and that in this case there is no redundancy due to radiance conservation, i.e., to replicate exactly the plenoptic function in a two-dimensional flat display we need all the information contained in a four-dimensional space.

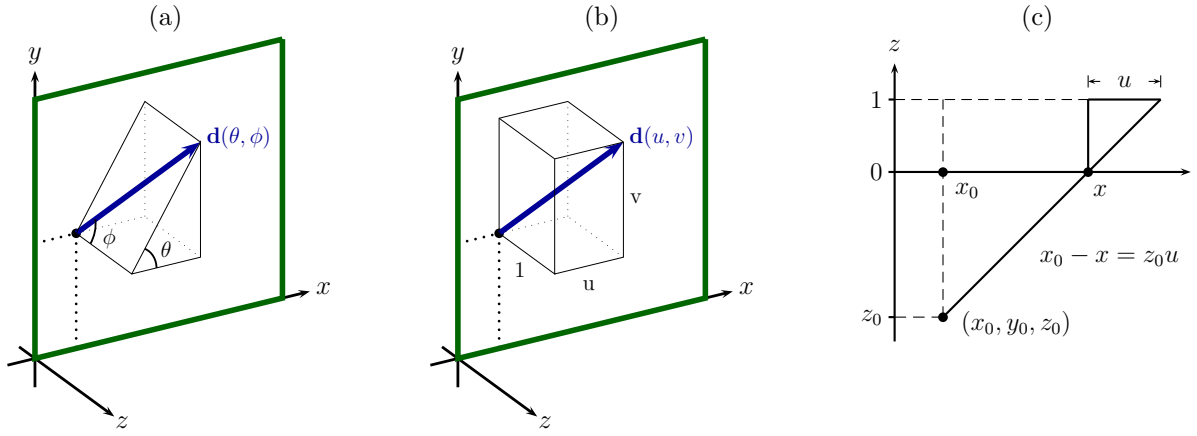

Figure 1. The spherical (a) and Cartesian (b) parameterizations of the plenoptic function in a display located at plane $z = 0$, and a diagram (c) showing why light from a point source at (x_0, y_0, z_0) define a line in the (x, u) space.

One advantage of defining the plenoptic function as $p_{\mathrm{a}}(x, y, \phi, \theta)$ is that we use the same angular variables as in the well-known spherical system of coordinates. However, there are also advantages of using the *Cartesian angular dimensions* (u, v), and defining the display's plenoptic function as

$$p_{\mathrm{d}}(x, y, u, v) \ : \ p_{\mathrm{d}}(x, y, \tan\phi\cos\theta, \tan\phi\sin\theta) = p_{\mathrm{s}}(x, y, \phi, \theta), \tag{3}$$

Fig. 1 (a) and (b) shows the two representations.

One advantage of this representation is that, from the basic geometry shown in Fig. 1(c), light emitted from a point source located at (x_0, y_0, z_0) maps to the following lines in the (x, u) and (y, v) spaces:

$$\begin{aligned} x + z_0 u &= x_0, \\ y + z_0 v &= y_0. \end{aligned} \tag{4}$$

It is possible to get a more intuitive understanding of the typical structure of $p_{\mathrm{d}}(x, y, u, v)$ by creating images where pixel color and brightness are defined by the values of the plenoptic function as we change variables in two chosen dimensions, while keeping the other dimensions at fixed values. For example, using α and β to represent constants, we can create spatial images from $p_{\mathrm{d}}(x, y, \alpha, \beta)$, which correspond to views from an orthographic camera if axes are properly scaled. Angular dimension images, defined as $p_{\mathrm{d}}(\alpha, \beta, u, v)$ correspond to images of perspective cameras with a pinhole at $(\alpha, \beta, 0)$, and film plane $z = 1$.

Mixed spatial and angular images, defined in the forms $p_{\mathrm{d}}(x, \alpha, u, \beta)$ and $p_{\mathrm{d}}(\alpha, y, \beta, v)$, are unusual, but as we show below, can be very useful for understanding the capabilities of 3-D displays. To start, let us consider how a display at $z = 0$ would recreate the plenoptic function defined by the set of objects in 3-D space shown in Fig. 2. Since we consider displays with only horizontal parallax, we constrain our analysis to images defined by (x, u) dimensions.

Fig. 3 shows three examples of spatial-angular images (with constants listed in the caption). We can observe that the most striking feature is that they are composed of nearly-constant-color areas, separated by what may seem like straight lines. Actually these may not be perfectly straight, but we know that they have to be composed of overlapping segments of straight lines, as defined by eq. (4), created by light emitted from surface points, beginning and ending at points (in the spatial-angular image) defined by occlusion between scene objects. Thus, the border points, defining color changes in the object's surface, or occlusion between objects, create the clearly visible transitions that are nearly straight.

We can also observe in Fig. 3 another fact predicted by eq. (4): the slope of the lines between regions is defined by the light source depth (z_0). Thus, red and black areas, defined by the cap that is located at positive z_0, has

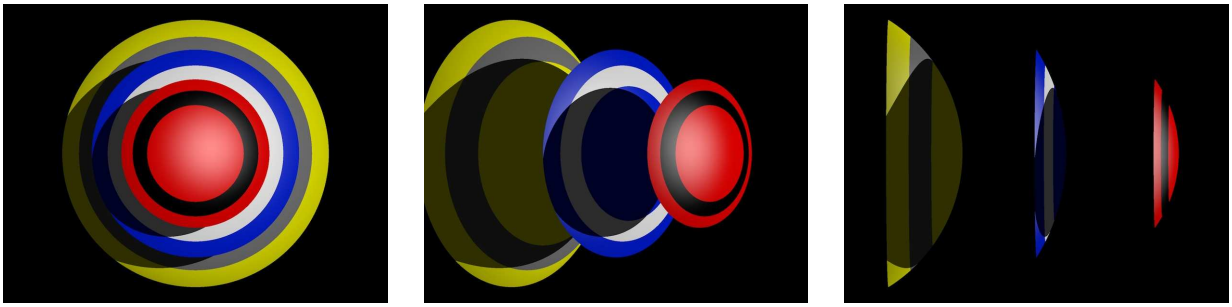

Figure 2. Frontal, 45° and 90° left-side views of the simulated set of three-dimensional objects used as example throughout this document. The three sphere caps have centers at line $x = y = 0$, and the base of the blue cap is in the display plane ($z = 0$).

Figure 3. Examples of spatial-angular images for a display at $z = 0$ reproducing views of the objects shown in Fig. 2. The horizontal direction corresponds to the spatial x dimension, and the vertical direction corresponds to the angular u dimension. (a) $p_{\mathrm{d}}(x, 0.25, u, 0)$; (b) $p_{\mathrm{d}}(x, 0.15, u, 0)$; (c) $p_{\mathrm{d}}(x, 0.15, u, 0.1)$.

transitions with negative slope; blue and white areas, corresponding to the blue cap at $z_0 \approx 0$ are separated by nearly vertical lines; the yellow and gray areas for the cap at negative z_0 create lines with positive slope.

This type of image had been observed and their properties had been discussed by several authors.[8–11] They are also known as epipolar images (EPI) in computer vision.[12]

In the next section we show the types of spatial-angular images that real displays can produce. To simplify the analysis, when we refer to a *spatial-angular image,* we mean the image created from the particular two-dimensional function

$$p_{\mathrm{h}}(x, u) = p_{\mathrm{d}}(x, 0, u, 0). \tag{5}$$

Furthermore, in all our spatial-angular images the horizontal direction corresponds to the spatial dimension (x), and vertical direction corresponds to the angular (u) dimension, with point $x = u = 0$ at the center of the image. Since nearly all our analysis is qualitative, the axes and their values, being the same for all images, are not shown.

Since practical displays cannot show an infinite amount of information, they must have light intensity nearly constant in discrete regions in the (x, y, u, v) space. We use the term *spatial resolution* to indicate (maybe roughly, when it is hard to define an exact value) how fine the discretization in the spatial x dimension is, and the term *angular resolution,* for the same in the angular u dimension.

Fig. 4 shows the two images that we use as reference, corresponding to objects shown in Fig. 2, as they would be produced by an ideal display at plane $z = 0$. On the left side we have a view from an orthographic camera oriented with a 15° angle from the z-axis. On the right we have $p_{\mathrm{h}}(x, u)$.*

*All images are better viewed in color and magnified in the electronic version of this document.

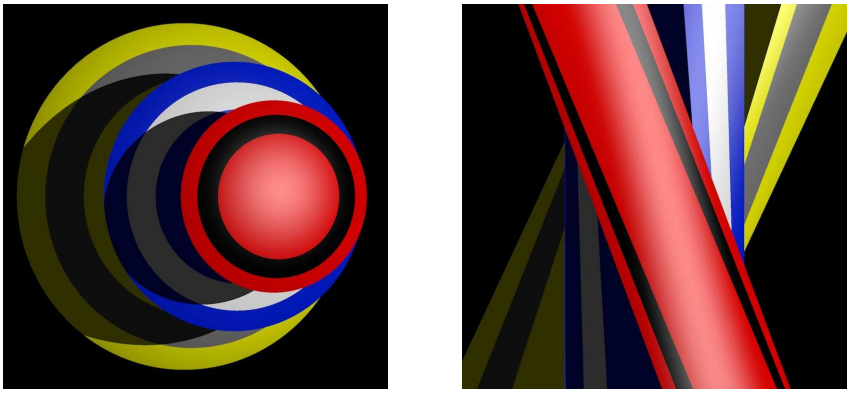

Figure 4. An ideal 3-D display recreating the arrangement of objects shown in Fig. 2 would show the spatial view on the left, and the spatial-angular view on the right. These images are used for comparisons with those from real displays.

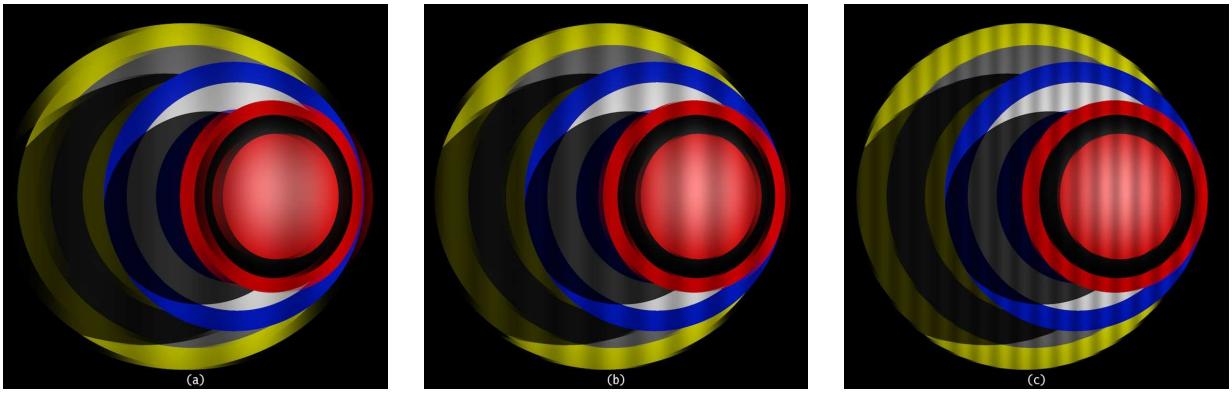

Figure 5. Views of scene recreated by displays implemented using anisotropic diffuser screen and multiple back-projectors. (a) 15 projectors; (b) 30 projectors; (c) 60 projectors.

3. APPLICATION TO 3-D DISPLAY ANALYSIS

Up to this point we have considered only the plenoptic function created by the objects in the 3-D scene we want to reproduce. An ideal display would recreate the same values, but current displays recreate only approximations. We analyze the quality of the approximation by simulating the display using ray-tracing,[13] and creating one spatial view and one spatial-angular image of the display.

3.1 Multiple projectors with anisotropic diffusers or with double lenticular arrays

The first type of display that we consider consists of multiple projectors arranged in an horizontal arc, projecting from behind onto a screen made of an anisotropic light diffuser, with wide diffusion along the vertical direction and very narrow diffusion along the horizontal direction (see Agócs *et al.*[14] for more details). This arrangement is very simple, and in a way very intuitive: light rays along different directions are generated by simply having light projected by different devices. To simplify this first analysis, we assume that each projected image has very high spatial resolution. Fig. 5 show views of simulations of this type of display, when using different number of projectors.

As we compare those images with the ideal in Fig. 4, we observe artifacts like line discontinuity/ghosting, and uneven brightness (increased in this example to be more visible). However, single images do not give any hint of how these artifacts change with viewer position. On the other hand, if we look at the corresponding spatial-angular images in Fig. 6, we can have an idea of what are the artifacts and how they change with viewer position, because these images do contain visual information about all the viewing angles.

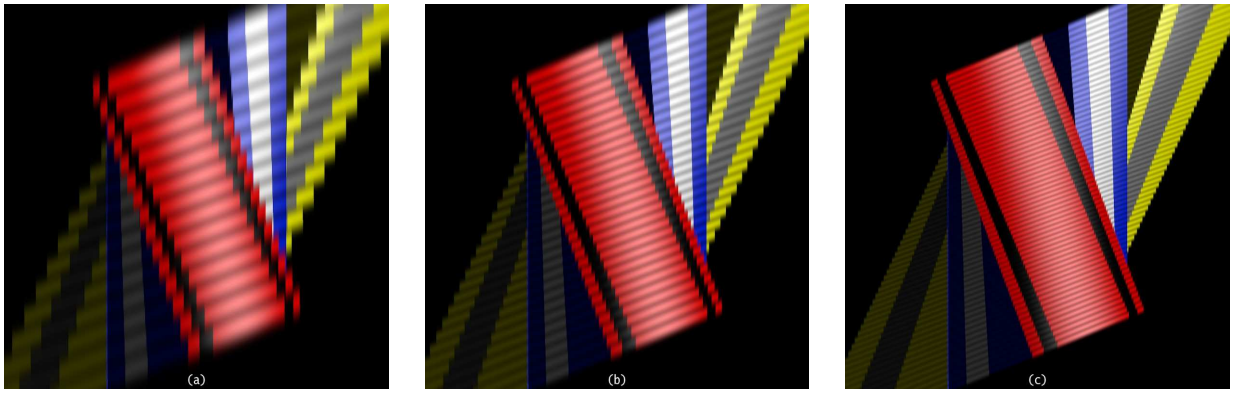

Figure 6. Spatial-angular images corresponding to displays implemented using an anisotropic diffuser screen and multiple back projectors. (a) 15 projectors; (b) 30 projectors; (c) 60 projectors.

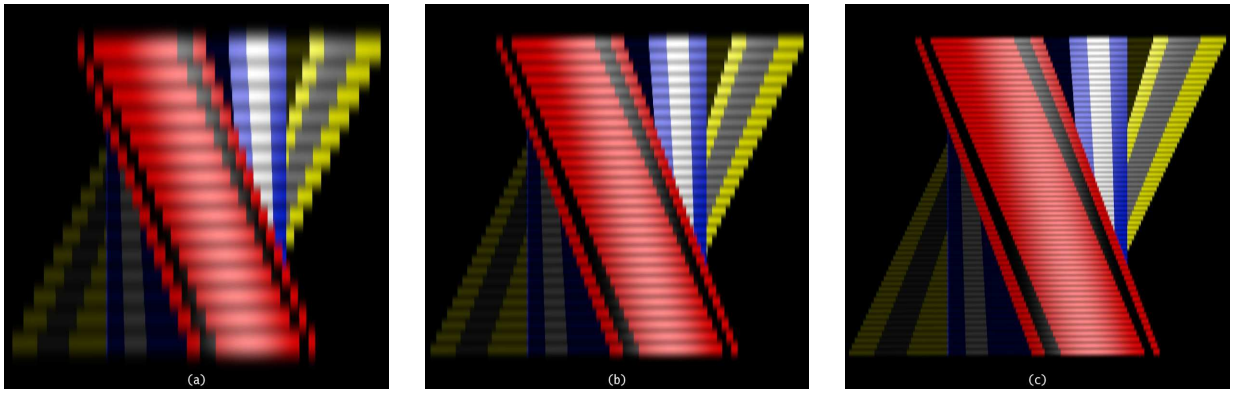

Figure 7. Spatial-angular images corresponding to displays implemented using a double-lenticular screen and multiple back projectors. (a) 15 projectors; (b) 30 projectors; (c) 60 projectors.

In addition we see in Fig. 4 a very clear pattern: we have "view patches" defined by each projector, with the diffusion at the screen (at depth $z = 0$) creating vertical lines of nearly-constant color. The width of the patch is defined by the type of anisotropic diffuser, which in turn is chosen to cover a field of view with a given number of projectors.

What is also clear, as we compare Fig. 6 with the reference in Fig. 4, is that in this method for 3-D display, we are in a sense trying to approximate slanted lines with segments of constant-length horizontal lines. Thus, objects near the display plane are very easy to approximate, while those that are further are increasingly more difficult. This idea is analyzed formally in Section 4. In this section we continue showing some more examples.

Fig. 7 shows spatial-angular images corresponding to a similar type of display, but in this case the viewer sees only the image from one projector at a time. This can be achieved using double-lenticular screens,[5,15] and Fig. 7 shows special cases when lens aberrations are ignored, and there is just the right amount of diffusion.[†] We observe that these images are similar to those of Fig. 6, with the main difference being how well they can approximate lines of different slopes.

3.2 Displays based on lenticular arrays

Another common type of 3-D display is composed of lens arrays, based in the idea of integral imaging, which has been studied since 1908.[16] Modern implementations[17,18] use projectors to generate dynamic images in the back of the lenses, enabling 3-D video.

[†]Views of a 3D screen from orthographic and perspective cameras differ in various aspects, but these are not important for the discussions in this paper.

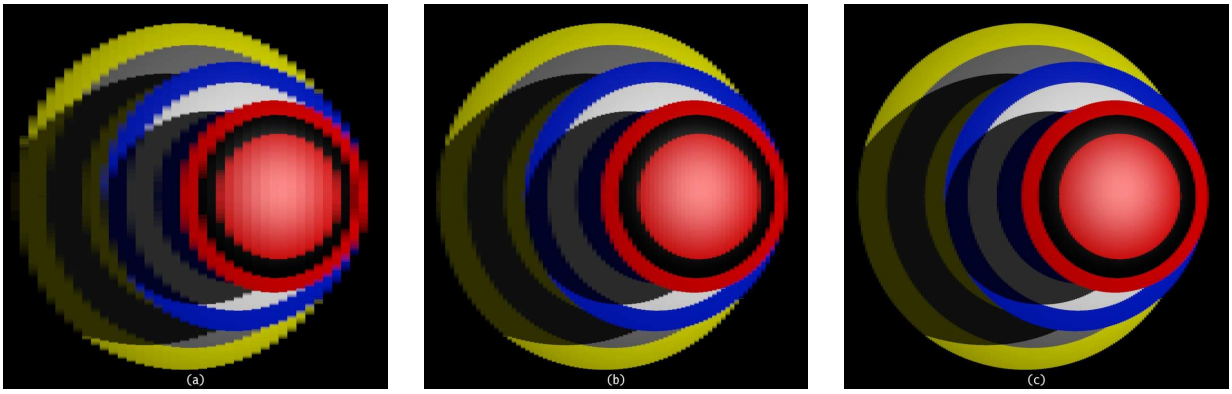

Figure 8. Views created by ideal lenticular arrays (without lens aberration), and a very large number of angular views, (a) lens size = 24 units; (b) lens size = 12 units; (c) lens size = 6 units.

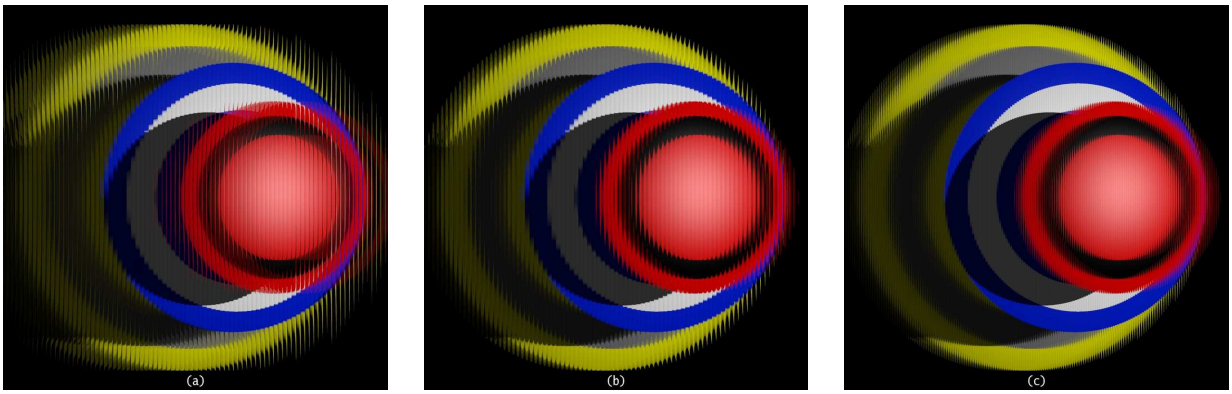

Figure 9. Views created by lenticular arrays with real lenses, very large number of angular views, (a) cross-sectional circular shape, lens size = 12 units; (b) improved shape, lens size = 12 units; (c) improved shape, lens size = 6 units.

We consider lenticular arrays, where vertical columns of lenses yield parallax in the horizontal direction only. Using simulations we analyze of visual quality by taking into consideration one design parameter at a time. First, let us assume that there is no lens aberration, i.e., all light rays that diverge from a point in the lens base (at focal depth) come out parallel. Furthermore, let us assume that the projected image in the base of the lens has extremely high resolution, so that a very large number of views is created.

Fig. 8 shows how the quality of views from such display would vary when we change the lens size. Several technical problems make it increasingly more difficult to create small lenticular lenses[19] and to project properly aligned high resolution images. However, the simulated views in Fig. 8 show that even in very favorable conditions image quality quickly degrades when the lenses are too large. (Cf. quality analysis in Section 4.)

We can add more realism to the simulations by considering real lenses, and Fig. 9 show examples of such views. Since lenses for displays need to cover wide viewing angles, lenses with top cross-sectional circular shape can degrade image quality substantially, as shown in Fig. 9 (a). Image quality can be improved significantly using other shapes, like elliptical,[19] but as shown in Figs. 9 (b) and (c), even when we change lens size some artifacts remain visible or blur the image.

Comparing images in Fig. 8 and Fig. 9, we can see that considering lens aberrations yields more realistic representations of the display, but do not really provide more insight into the very basic characteristics of this type of display. It is more to interesting analyze how we can pre-process the images under each lens to improve quality. Fig. 10 shows spatial-angular diagram defined by different lens sizes and pre-processing methods. Before discussing these resolution aspects, it is interesting to comment on another useful feature of spatial-angular

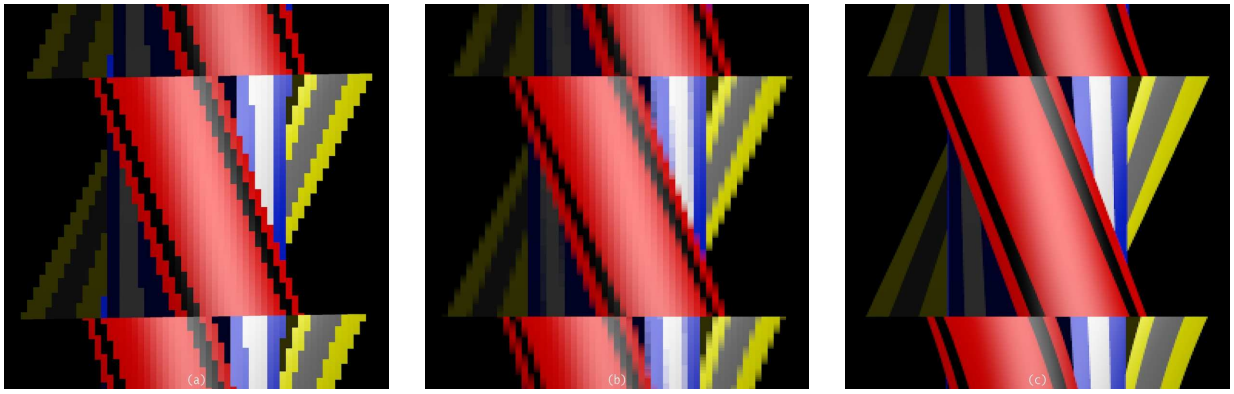

Figure 10. Spatial-angular images of lenticular array display, using different anti-aliasing methods. (a) lens size = 24 units, unfiltered sampling; (b) lens size = 24 units, spatial average; (c) lens size = 6 units, spatial average;

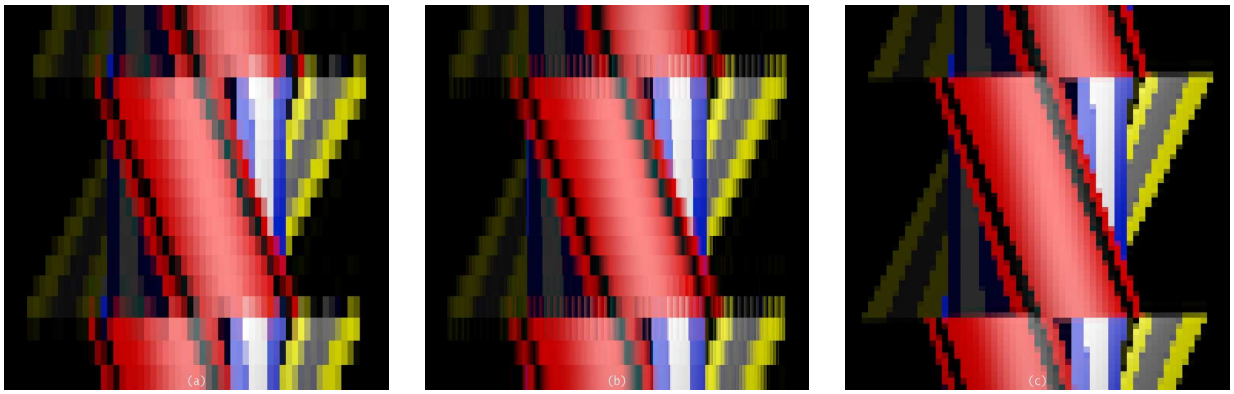

Figure 11. Spatial-angular images of lenticular array display, when resolution along the spatial and angular dimensions are of nearly same magnitude. (a) lens size = 24 units, 12 views; (b) lens size = 6 units, 12 views; (c) lens size = 24 units, 48 views

images: the repetition seen in the top and bottom of those images is the well-known "flipping" that occurs on this type of display when it is observed from an angle that is too large.

As shown in Fig. 10 (a), if we create each view independently, we can have as much resolution as provided by the lens size, but we observe discontinuities as we change the viewing direction u, which means that displayed edges "jump" as the viewer moves. For the same lens size, these artifacts can can be reduced by smoothing the transition between views, as shown in Fig. 10 (b). However, this also has the disadvantage of blurring the views. The amount of blur depends on the lens size, and Fig. 10 (c) shows that only smaller lenses would allow both smoother transitions and crisp images.

The next factor to be considered is the resolution of the image projected under each lens. We assume that the diffuser is exactly at focal length, and thus, in the image under each lens, regions of constant color in the direction perpendicular to the lens axis define regions of constant color along the u axis in the spatial-angular images. Displays that have extremely small lens size, such that the spatial resolution is much higher than the angular resolution, produce spatial-angular images that look like those in Fig. 7. Fig. 11 shows examples of what happens when the spatial and angular resolutions are of nearly same magnitude: in the spatial-angular image we observe regions of identical color as rectangles.

4. MEASURING THE VIEW QUALITY

Perception of three-dimensional depth is defined, by a significant amount, through cues on how occlusions change with viewer position. This fact motivates us, as we look for ways to measure quality of 3-D displays, to consider

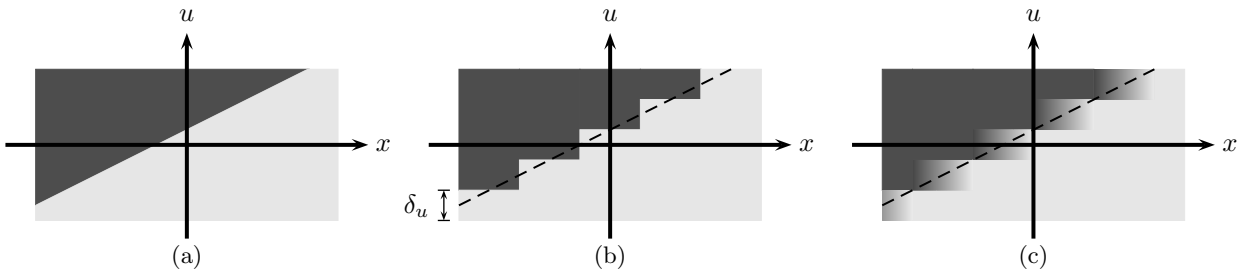

Figure 12. Spatial-angular images with gray values representing different values of luminance. (a) Original, defined by a single boundary discontinuity; (b) Discrete approximation with ideal diffuser; (c) Continuous approximation with ideal diffuser.

as the basic model and reference the simplest type of occlusion: a half-plane with a vertical edge and constant radiance, in front of a constant-radiance infinite background.

The plenoptic function in the display showing this single vertical depth discontinuity, at $z = z_0$, is

$$p_{\mathrm{d}}(x, y, u, v) = p_{\mathrm{h}}(x, u) = \begin{cases} p_a, & x + z_0 u \geq x_0, \\ p_b, & \text{otherwise}, \end{cases} \tag{6}$$

where p_a and p_b are the radiance values of the plane and background. This spatial-angular image is shown in Fig. 12(a), where different gray levels represent the two radiance values.

The first type of display we study is when the spatial resolution is much higher than angular resolution. This can occur with the type of display used as example in Section 3.1, and is shown in the spatial angular images of Fig. 7. To simplify notation we assume that angular resolution is defined by a step size δ_u, and that spatial resolution is infinite. Under these conditions, the function that best approximates $p_{\mathrm{h}}(x, u)$ in a discrete manner is shown in Fig. 12(b), defined by

$$r_{\mathrm{h}}(x, u) = \begin{cases} p_a, & x + z_0\, Q_{\delta,\epsilon}(u) \geq x_0, \\ p_b, & \text{otherwise}. \end{cases} \tag{7}$$

where we have a quantization function

$$Q_{\delta,\epsilon}(u) = \delta \left\lfloor \frac{u - \epsilon}{\delta} + \frac{1}{2} \right\rfloor + \epsilon, \tag{8}$$

with step size δ and offset ϵ. Note that ϵ only changes the position of the transitions, but not the quality of the approximation.

In displays with anisotropic diffusers $1/\delta_u$ is directly proportional to the number of projectors, and in lenticular array displays it is directly proportional to the number of pixels under each lens.

There is still no agreed method for measuring errors in the plenoptic function reproduction. Defining a general *distortion function* $D(a, b)$ to measure the error between radiance values a and b, one approach to define overall distortion (or error) is to integrate along the spatial dimension, and take averages along the angular dimension—equivalent in a sense to taking average among views. Applying this definition to the approximation defined by eq. (7), we obtain[‡]

$$\bar{E}_d = \lim_{U \to \infty} \frac{1}{2U} \int_{-U}^{U} \int_{-\infty}^{\infty} D(p(x, u), r_d(x, u))\, \mathrm{d}x\, \mathrm{d}u = |z_0|\, \delta_u\, \frac{D(p_a, p_b) + D(p_b, p_a)}{8}. \tag{9}$$

It is interesting to see that, from this very simple model and analysis, we can conclude that the quality measure depends on the relative depth ($|z_0|$) of the displayed object. This fact can be empirically observed 3-D

[‡]Note that we do not assume that $D(a, b) = D(b, a)$.

displays prototypes, but it is easy to be confused about what exactly is causing the distortion. For example, one could have guessed that lens aberration were the main cause, but this shows that we reach the same conclusion with ideal lenses.

Another option is to use the average luminance value for choosing the approximation, as shown in Fig. 12(c), using the definition

$$r_c(x,u) = \begin{cases} p_a, & x + z_0\, Q_{\delta,\epsilon}(u) \geq x_0 + |z_0|\delta/2, \\ p_b, & x + z_0\, Q_{\delta,\epsilon}(u) \leq x_0 - |z_0|\delta/2, \\ \dfrac{p_a + p_b}{2} + \dfrac{(p_a - p_b)(x - x_0 + z_0 Q_{\delta,\epsilon}(u))}{|z_0|\delta}, & \text{otherwise.} \end{cases} \tag{10}$$

In this case the total distortion is

$$\begin{aligned} \bar{E}_c &= \lim_{U\to\infty} \frac{1}{2U} \int_{-U}^{U} \int_{-\infty}^{\infty} D(p(x,u), r_c(x,u))\, \mathrm{d}x\, \mathrm{d}u \\ &= |z_0|\, \delta_u \int_0^1 \left[tD(p_a, tp_a + (1-t)p_b) + (1-t)D(p_b, tp_a + (1-t)p_b) \right]\, \mathrm{d}t, \end{aligned} \tag{11}$$

When we use distortion measure $D(x,y) = |x-y|^k$ we obtain

$$\bar{E}_d = \frac{1}{4}\, |z_0|\, \delta_u\, |p_a - p_b|^k, \qquad \bar{E}_c = \frac{2}{(k+1)(k+2)}\, |z_0|\, \delta_u\, |p_a - p_b|^k. \tag{12}$$

Another measure of distortion that can be of interest is the spatial displacement of the occlusion discontinuity. It can be shown that the average of the distance between real and reproduced edge, raised to power k, is

$$\bar{d}_k = \frac{1}{k+1} \left| \frac{z_0 \delta_u}{2} \right|^k, \tag{13}$$

which again depends on object depth $|z_0|$.

A second case to consider is when angular resolution is much higher than spatial resolution. The results are very similar, since we in a way just have to rotate the graphs in Fig. 12 by 90°, and replace δ_u by δ_x. However, since averages are still taken over all views, the distortion and error results are similar, but correspond to actually replacing $\delta_u|z_0|$ with δ_x.

Distortion values for the case when the spatial and angular resolutions have similar magnitudes do not have simple formulas, but some aspects can be inferred from conclusions from the two extreme cases presented above.

5. IMPROVING BOTH SPATIAL AND ANGULAR RESOLUTION WITH MULTIPLE PROJECTORS

What we see in the case of multiple projectors with double-lenticular or anisotropic diffuser screens is that spatial resolution is defined by the resolution of each projector, while angular resolution is directly proportional to the number of projectors. Thus, the only way to increase, with the same quality, the usabnle depth range of virtual objects or the usable range of viewing angles, is to use more projectors. Conventional displays with lenticular lens arrays, on the other hand, have angular resolution controlled by the resolution of images under each lens, but spatial resolution can only be increased by reducing lens size. What is missing is a way to have more flexibility in the control of the spatial and angular resolutions without using very large number of projectors or extremely small lenses.

We propose a method to achieve this goal by in a sense combining the two approaches. Let us consider the diagram on the left of Fig. 13. Systems that basically implement Lippmann's[16] ideas, only adding projectors to control the image under each lens, use wide-angle diffusers.[17,18] Thus, using more projectors, with different incident angles, does not improve quality because the light of all projectors is mixed together. However, if

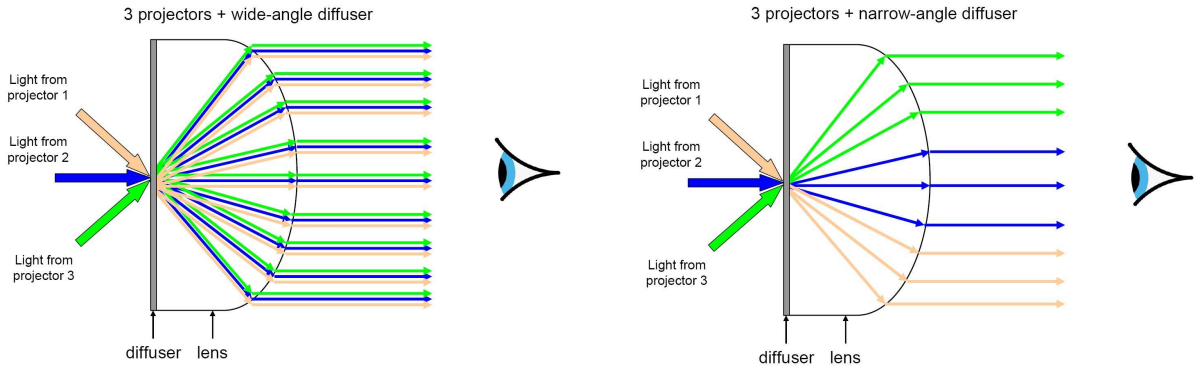

Figure 13. Diagrams showing how to use multiple projectors to increase the spatial resolution of 3-D displays based on lenticular lens arrays. Conventional system on the left combines the light of all projectors, while proposed system on the right uses different incident angles to have light coming out of different parts of the lens.

narrow-angle diffusers[§] are used, light from each projector comes out of different spatial position in the surface of the lens. Since the pixels come from different projectors, we can choose different colors, effectively increasing the spatial resolution of the display.

Fig. 14 show examples of simulations, *using real lenses* with improved cross-section (not circular). Fig. 14(a) shows the conventional system, with a single projector and wide-angle diffuser, and artifacts due to lens aberration. Fig. 14(b) is shown just to illustrate the variables involved: if we use several projectors, and very narrow diffuser angles, each projector creates a thin vertical line, and their combination does not cover the whole display surface. On the other hand, since each line uses only a part of the lens surface, lens aberration is much less of a problem. Fig. 14(c) shows what happens when we have more projectors and wider diffuser angle: the whole display surface is covered with overlapping lines, creating a continuous image.

At this point one may wonder if the technique works only for some views. We can find the answer observing Fig. 15, which shows the corresponding spatial-angular images for each display. We can see in Fig. 15(c) that, not only the images for different angles are also nearly full, this new configuration can avoid (to some extent) the repetition of the views. Furthermore, comparing images Fig. 4 with those in Figs. 14 and 15 (a) and (c), we conclude that spatial resolution has increased significantly.

The condition to obtain this improvement is that we must know the mapping of each projector pixel to the 4D light ray it generates on the display surface, to correctly compute the pixel color and brightness. Fortunately, automatic multi-display calibration is an active area of research, and sub-pixel accuracy has been reported.[20]

The fact that, in the proposed configuration, light from each projector is deflected by only part of the lens surface, raises the question of whether there are advantages of using more unconventional optical elements. For instance, Fig. 16 shows view and spatial-angular images of a display where lenticular array was replaced by optics with top cross-section of sinusoidal shape, i.e., an optical system that is definitely non-conventional.

It is important to note that these examples are meant to only show that there can be advantages in this new type of display. Methods to define the optimal number and arrangement of projectors/diffusers is outside the scope of this paper.

6. CONCLUSIONS

In this work we present some contributions for better understanding the most fundamental factors that define the visual quality of displays meant to reproduce light fields. In addition, we show how a new type of display arrangement, using multiple projectors, can give designers much greater flexibility in increasing both the spatial and angular resolution of 3-D displays.

[§]Anisotropic diffusers are needed for systems with only horizontal parallax.

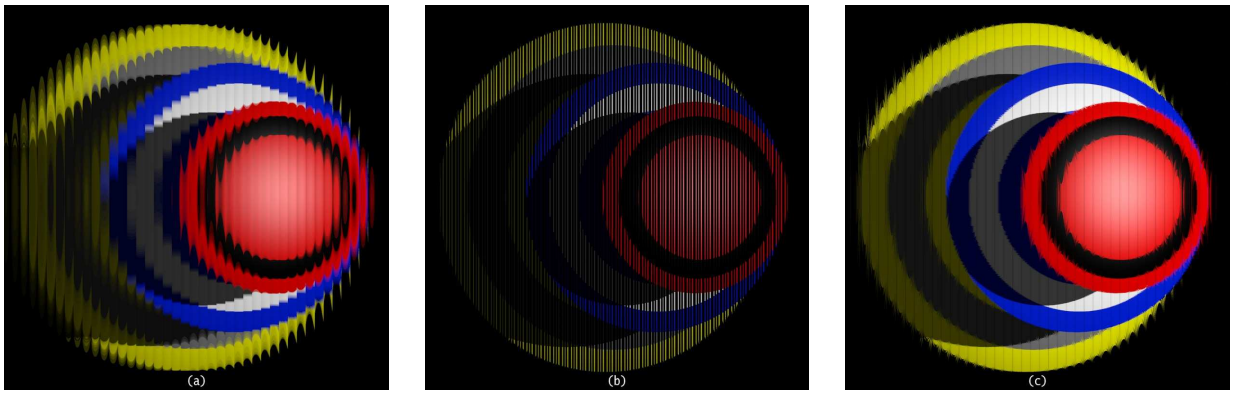

Figure 14. Example of how spatial resolution can be increased using multiple projectors. (a) lens size = 24 units, one projector and 90° diffuser; (b) lens size = 24 units, 4° diffuser, 4 equally-spaced projectors; (c) lens size = 24 units, 8° diffuser, 15 equally-spaced projectors.

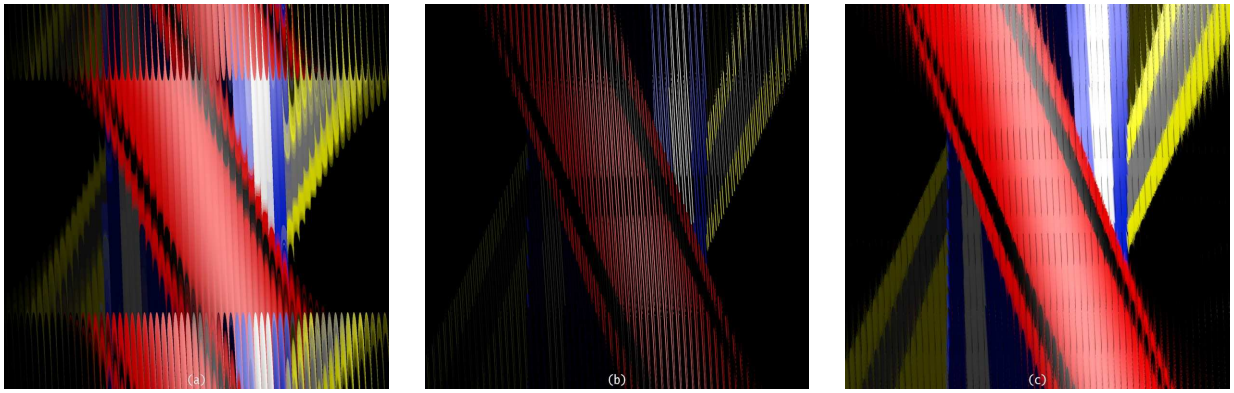

Figure 15. Spatial-angular images of the displays corresponding to the views shown in Fig. 14.

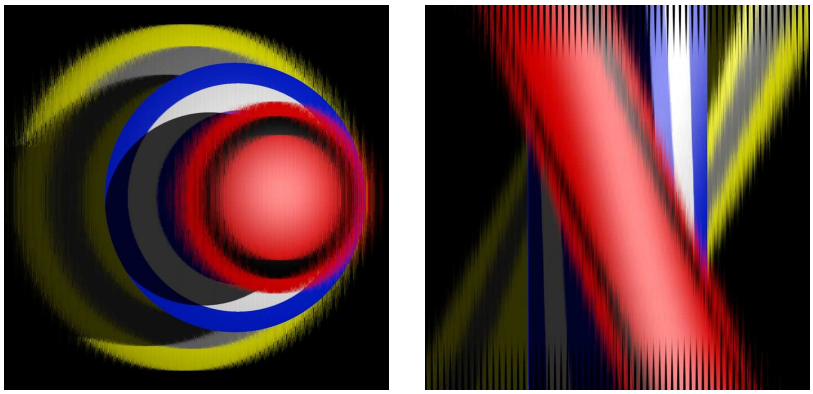

Figure 16. Images generated with display using non-conventional optics.

We show how images created by selecting one spatial and one angular dimension of the four-dimensional plenoptic function, which we call spatial-angular images, can provide insight into the limitations of current displays. We present a variety of images of simulated display views, in some common display types, and with several configurations or display parameters. These examples provide motivation for mathematical analysis, where we consider some measures of distortion for the case of one half-plane occlusion. With this simple model we can demonstrate, for example, a basic property of all 3-D displays, which is how limited angular resolution defines a loss of quality that depends on reproduced object's depth, compared to display plane.

We also consider that, in standard configurations, displays using lens arrays can only improve spatial resolution by using smaller lenses, while displays using multiple projectors can only improve angular resolution by increasing the number of projectors. We show that, using controlled light diffusion, it is possible to create a hybrid scheme, employing both multiple projectors and lens arrays, which can increase spatial resolution beyond the previous limit defined by lens size, and also increase angular resolution with higher projected image resolution, instead of more projectors. Simulations and spatial-angular images of the proposed scheme show that, given correct projector calibration, the proposed method can effectively improve spatial and angular resolution, increase field of view, and reduce lens aberration effects.

REFERENCES

[1] T. Okoshi, *Three-Dimensional Imaging Techniques*, Academic Press, New York, NY, 1976.

[2] T. Okoshi, "Three-dimensional displays," *Proceedings of the IEEE* **68**, pp. 548–564, May 1980.

[3] I. Sexton and P. Surman, "Stereoscopic and autostereoscopic display systems," *IEEE Signal Processing Magazine* **16**, pp. 85–99, May 1999.

[4] B. Javidi and F. Okano, eds., *Three-Dimensional Television, Video, and Display Technologies*, Springer, Berlin, Germany, 2002.

[5] N. A. Dodgson, "Autostereoscopic 3d displays," *IEEE Computer* **38**, pp. 31–36, Aug. 2005.

[6] P. Benzie, J. Watson, P. Surman, I. Rakkolainen, K. Hopf, H. Urey, V. Sainov, and C. von Kopylow, "A survey of 3DTV displays: Techniques and technologies," *IEEE Transactions on Circuits and Systems for Video Technology* **17**, pp. 1647–1658, Nov. 2007.

[7] M. Levoy, "Light fields and computational imaging," *IEEE Computer* **39**, pp. 46–55, Aug. 2006.

[8] E. H. Adelson and J. R. Bergen, "The plenoptic function and the elements of early vision," in *Computational Models of Visual Processing*, M. Landy and J. Movshon, eds., ch. 1, pp. 3–20, MIT Press, Cambridge, MA, 1991.

[9] E. Camahort and D. Fussell, "A geometric study of light field representations," Technical Report TR99-35, Department of Computer Sciences, The University of Texas at Austin, 1999.

[10] J.-X. Chai, X. Tong, S.-C. Chan, and H.-Y. Shum, "Plenoptic sampling," in *SIGGRAPH'00: Proceedings of the 27th annual conference on computer graphics and interactive techniques*, pp. 307–318, ACM Press/Addison-Wesley Publishing Co., (New York, NY, USA), 2000.

[11] C. Zhang and T. Chen, "Non-uniform sampling of image-based rendering data with the position-interval error (PIE) function," in *Proceedings SPIE Vol. 5150: Visual Communication and Image Processing*, **3**, pp. 1347–1358, 2003.

[12] R. C. Bolles, H. H. Baker, and D. H. Marimont, "Epipolar-plane image analysis: An approach to determining structure from motion," *International Journal of Computer Vision* **1**, pp. 7–55, June 1987.

[13] M. Pharr and G. Humphreys, *Physically Based Rendering: from Theory to Implementation*, Morgan Kaufmann Publishers, 2004.

[14] T. Agócs, T. Balogh, T. Forgács, F. Bettio, E. Gobbetti, G. Zanetti, and E. Bouvier, "A large scale interactive holographic display," in *Proceedings of the IEEE Virtual Reality Conference: Workshop on Emerging Display Technologies*, pp. 2–3, Mar. 2006.

[15] W. Matusik and H. Pfister, "3D TV: a scalable system for real-time acquisition, transmission, and autostereoscopic display of dynamic scenes," in *Proceedings ACM International Conference on Computer Graphics and Interactive Techniques (SIGGRAPH)*, pp. 814–824, 2004.

[16] G. Lippmann, "Épreuves réversibles. photographies intégrales," *Comptes rendus de l'Académie des Sciences* **146**, pp. 446–451, Mar. 1908.

[17] H. Liao, M. Iwahara, N. Hata, and T. Dohi, "High-quality integral videography using a multiprojector," *Optics Express* **12**, pp. 1067–1076, Mar. 2004.

[18] R. Yang, X. Huang, S. Li, and C. Jaynes, "Toward the light field display: autostereoscopic rendering via a cluster of projectors," *IEEE Transactions on Visualization and Computer Graphics* **14**, pp. 84–96, Jan. 2008.

[19] R. B. Johnson and G. A. Jacobsen, "Advances in lenticular lens arrays for visual display," in *Proceedings of SPIE: Current Developments in Lens Designa and Optical Engineering*, **5874**, SPIE, Aug. 2005.

[20] H. Chen, R. Sukthankar, G. Wallace, and T. jen Cham, "Calibrating scalable multi-projector displays using camera homography trees," in *Proceeding of the IEEE Conference on Computer Vision and Pattern Recognition*, pp. 9–14, 2001.